COVERSHEET

Peer Review Status Statement

This is a non-peer-reviewed preprint submitted to EarthArXiv.

The manuscript has not been submitted to any journal for peer review at the time of this submission (2026-05-27). A revised version may be submitted to a peer-reviewed journal in the future.

Title

R-critical constraints on relamination efficiency: The role of mechanical coupling in continental crust recycling

---

Authors

Shizhong Chen[1,2*] **Xingxing Duan**[1,2]

[1] Urumqi Natural Resources Survey, China Geological Survey, China

[2] Innovation Base of Metallogenic Prediction and Prospecting in Central Asia Orogenic Belt, China

*Corresponding author: nanjingcsz@qq.com

ORCID: 0000-0001-7527-1452

Co-author: 86000536@qq.com

ORCID: 0009-0006-1017-8373

Date of Submission

2026-05-27

AI Assistance Disclosure

During the preparation of this work, the authors used Kimi K2.6 (Moonshot AI) for code implementation assistance and language polishing only. All scientific hypotheses, theoretical framework development (including the R-critical concept, efficiency curves, and phase diagram design), data interpretation, and

conclusions were independently developed by the authors. The authors take full responsibility for the scientific content.

Data and Code Availability

All numerical simulation code, input parameters, and figure generation scripts used in this study are available at: - GitHub: https://github.com/peter-clogite/R_Critical_Relamination - Zenodo archive: https://doi.org/10.5281/zenodo.20446104
The code is released under the MIT License.

Competing Interests

The authors declare no competing financial interests.

Funding

This work was supported by the Regional Collaborative Innovation Special Project (Science and Technology Assistance Program for Xinjiang) and the Key Research and Development Program of Xinjiang Uygur Autonomous Region, under Grant Nos. 2026E02012 and 2024B03009, respectively. The funders had no role in study design, data collection and analysis, decision to publish, or manuscript preparation.

Version History

- **v1.0** (2026-05-27): Initial preprint submission
- **v2.0** (2026-05-27): Corrected formula rendering, updated references, removed erroneous DOIs
- **v2.1** (2026-05-27): Cleaned formatting, removed watermark artifacts
- **v2.2** (2026-05-27): Reorganized figure placement (inline format), corrected Gerya et al. citation year (2004)

Mastodon Handle

Not provided.

This coversheet is prepared in accordance with EarthArXiv submission guidelines (https://eartharxiv.github.io/resources/PeerStatus.pdf).

R-critical constraints on relamination efficiency: The role of mechanical coupling in continental crust recycling

Shizhong Chen[1,2*] Xingxing Duan[1,2]

[1] Urumqi Natural Resources Survey, China Geological Survey, China

[2] Innovation Base of Metallogenic Prediction and Prospecting in Central Asia Orogenic Belt, China

*Corresponding author: nanjingcsz@qq.com (S. Chen); ORCID: 0000-0001-7527-1452

Co-author: 86000536@qq.com (X. Duan); ORCID: 0009-0006-1017-8373

ABSTRACT

Relamination—the reincorporation of deeply subducted continental crust into the overriding plate—has been proposed as a major mechanism for continental growth and differentiation. While numerical models and high-pressure experiments demonstrate the thermochemical feasibility of this process, a fundamental question remains: under what mechanical conditions is relamination sufficiently efficient to produce geochemically detectable hybrid melts? Here we introduce the R-critical dimensionless parameter, defined as the ratio between buoyancy-driven mixing forces and viscous resistance at the crust–mantle interface. R-critical quantifies the mechanical coupling required for efficient hybridization of crustal fragments within peridotite matrix. Our analysis demonstrates that relamination efficiency is not solely governed by pressure–temperature conditions, but fundamentally constrained by interface viscosity, density contrast, strain rate, and fragment size. When the mechanical coupling parameter R falls below the critical threshold (R-critical), hybrid melting becomes physically inhibited regardless of experimental temperature or pressure, implying that global relamination fluxes may be substantially lower than previously estimated. This framework provides a quantitative discriminator between relamination and delamination, and offers testable predictions for seismic

anisotropy, UHP terrane deformation structures, and post-collisional magmatic signatures.

Keywords: relamination; continental crust recycling; mechanical coupling; R-critical; subduction; hybrid melting; crust-mantle interface; geodynamic modeling

---

1. INTRODUCTION

1.1 Background

The recycling of continental crust into the mantle and its subsequent return to the crust—processes collectively termed relamination—has gained increasing attention as a fundamental mechanism of continental evolution (Hacker et al., 2011; Gerya et al., 2004). During continental collision, deeply subducted crustal fragments may detach from the downgoing slab and ascend into the mantle wedge, where they interact with peridotite to produce hybrid magmas. These hybrid melts, enriched in crustal signatures, are thought to contribute significantly to post-collisional magmatism and continental growth.

Recent advances in thermomechanical modeling have demonstrated that relamination can reproduce first-order natural observations, including the temporal lag between collision and post-collisional magmatism, and the characteristic geochemical signatures of collision-related igneous rocks (Gómez-Frutos et al., 2026). High-pressure experiments have further validated that crustal compositions, when mixed with peridotite at appropriate pressure–temperature conditions, can indeed generate hybrid melts with geochemically meaningful signatures.

1.2 The Missing Link: Mechanical Coupling

Despite these advances, a critical gap persists between numerical models and experimental petrology. Numerical models output pressure–temperature–time (P–T–t) trajectories and deformation geometries, while experiments require pre-homogenized mixtures as input. The physical process bridging these two scales—mechanical mixing at the discrete crust-mantle interface—has not been quantitatively addressed.

Natural relamination involves discrete crustal fragments interacting with peridotite matrix, not the homogeneous mixtures used in experiments. The transition from discrete fragments to hybrid mixtures is governed by mechanical coupling at the crust-mantle interface. Without sufficient mechanical coupling, the experimental starting conditions may never be achieved in nature, regardless of how favorable the P–T conditions appear.

1.3 The R-critical Framework

In this study, we introduce the R-critical dimensionless parameter to quantify the mechanical coupling required for efficient hybridization. Drawing analogy from classical dimensionless numbers in fluid and solid mechanics (e.g., Reynolds number, Rayleigh number), R-critical provides a first-order physical threshold for determining when mechanical mixing can bridge the gap between numerical model outputs and experimental inputs.

Our central hypothesis is that relamination efficiency is fundamentally constrained by mechanical coupling, and that many natural scenarios may fall below the critical threshold required for efficient hybridization. This implies that global relamination fluxes—and consequently the contribution of relamination to continental growth—may be substantially lower than previously estimated.

---

2. METHODS

2.1 Definition of the R-critical Parameter

The R-critical parameter is defined as the ratio between the characteristic buoyancy force driving mechanical mixing and the viscous resistance opposing it at the crust-mantle interface:

$$R = \frac{F_b}{F_v} = \frac{\Delta\rho \cdot g \cdot L^3}{\eta_i \cdot \dot{\varepsilon} \cdot L^2} = \frac{\Delta\rho \cdot g \cdot L}{\eta_i \cdot \dot{\varepsilon}}$$

Where: - $\Delta\rho$ = density contrast between crustal fragment and mantle (kg/m³) - g = gravitational acceleration (9.81 m/s²) - L = characteristic fragment size (m) - η_i = effective viscosity of the crust-mantle interface (Pa·s) - $\dot{\varepsilon}$ = characteristic strain rate (s^{-1})

This formulation captures the competition between buoyancy-driven ascent and viscous resistance to deformation and mixing.

2.2 Critical Threshold

The critical threshold R-critical is determined by the minimum mechanical coupling required to achieve the hybrid mixing ratios (X_b) observed in natural composite dikes and experimental products. Based on the analysis of Vogt et al. (2013), who documented composite dike mixing ratios in the range X_b = 0.4–0.8, we adopt a reference value of:

$$R_{critical} = 10.0$$

This value represents the threshold above which mechanical coupling is sufficient to produce the mixing ratios required for geochemically detectable hybridization.

2.3 Efficiency Model

Relamination efficiency (E) is modeled as a sigmoidal function of the normalized parameter $R/R_{critical}$:

$$E = \frac{1}{1 + \exp\left(-\frac{R/R_{critical} - 1}{w}\right)}$$

Where w = 0.3 controls the width of the transition zone. This formulation provides a smooth transition between inefficient ($E \approx 0$) and efficient ($E \approx 1$) relamination regimes, avoiding the unphysical discontinuity of a step function. Alternative formulations (linear and step-function) are provided for comparison and sensitivity analysis.

2.4 Parameter Ranges and Sources

All physical parameters are constrained by published experimental and observational data:

Parameter	Symbol	Range	Best Estimate	Source
Density contrast	$\Delta\rho$	200–500 kg/m³	300 kg/m³	Crust/mantle density difference (Christensen &

Parameter	Symbol	Range	Best Estimate	Source
				Mooney, 1995)
Interface viscosity	η_i	10^{17}–10^{21} Pa·s	10^{18} Pa·s	Rock deformation experiments (Hirth & Kohlstedt, 2003)
Strain rate	$\dot{\varepsilon}$	10^{-16}–10^{-12}s^{-1}	10^{-14} s^{-1}	GPS measurements (Kreemer et al., 2014)
Fragment size	L	10^{3}–10^{5} m	5×10^{3} m	Seismic tomography / Field mapping

2.5 Numerical Implementation

All calculations were implemented in Python 3.9+ using NumPy and SciPy libraries. The code is structured as follows: 1. Core module (r_critical.py): Computes R and E for given parameter sets. 2. Efficiency module (efficiency_model.py): Generates efficiency curves across parameter sweeps. 3. Phase diagram module (phase_diagram.py): Produces 2D phase diagrams in parameter space.

Unit tests verify asymptotic behavior, monotonicity, and consistency with analytical solutions for simplified cases.

3. RESULTS

3.1 R-critical Definition and Physical Interpretation

Figure 1 illustrates the physical meaning of R-critical. The crust-mantle interface acts as a rheological boundary where buoyancy forces (driving mixing) compete with viscous forces (resisting mixing). When $R > R_{critical}$, the interface is sufficiently weak to allow mechanical coupling and hybridization. When $R < R_{critical}$, the interface remains too strong, and discrete crustal fragments ascend without significant mixing.

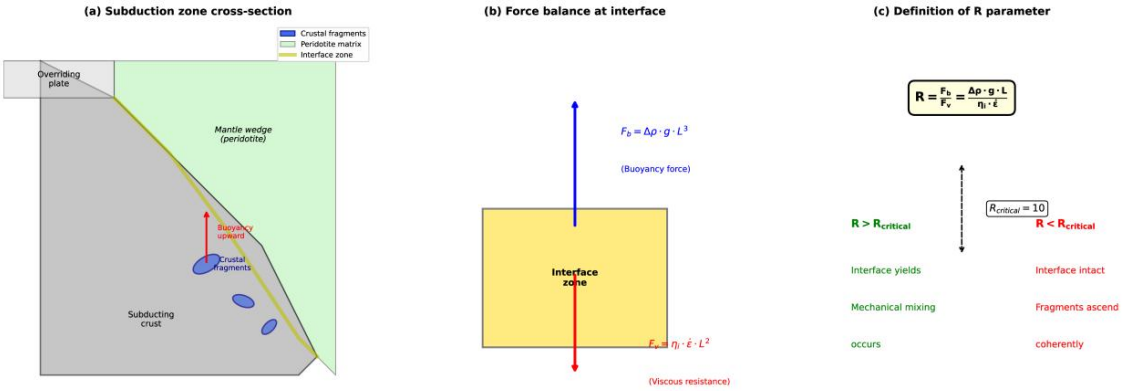

Figure 1. The R-critical parameter and mechanical coupling at the crust–mantle interface. (a) Subduction zone cross-section showing discrete crustal fragments (blue ellipses) embedded in peridotite matrix (green). The crust–mantle interface (yellow highlight) marks the zone of mechanical interaction where buoyancy-driven ascent competes with viscous resistance. The overriding plate (light grey) and subducting slab (dark grey) provide the tectonic framework. Red arrows indicate buoyancy-driven upward motion of crustal fragments. (b) Force balance at the interface. The interface zone (yellow block) experiences upward buoyancy force $F_b = \Delta\rho \cdot g \cdot L^3$ (blue arrow) and downward viscous resistance $F_v = \eta_i \cdot \dot{\varepsilon} \cdot L^2$ (red arrow). The dimensionless parameter $R = F_b/F_v$ quantifies their competition. (c) Definition of the R parameter and its physical interpretation. The central equation $R = (\Delta\rho \cdot g \cdot L)/(\eta_i \cdot \dot{\varepsilon})$ defines the mechanical coupling strength. When $R > R_{critical}$ (green zone), the interface yields and mechanical mixing occurs. When $R < R_{critical}$ (red zone), the interface remains intact and fragments ascend as coherent blocks. The reference threshold $R_{critical} = 10.0$ is calibrated against natural composite dike mixing ratios (Vogt et al., 2013).

3.2 Efficiency Curves

Figure 2 presents efficiency curves generated by systematic parameter sweeps. Key observations:

1. **Viscosity sensitivity:** Efficiency drops sharply as interface viscosity increases above 10^{19} Pa·s, even for favorable values of other parameters.

2. **Fragment size effect:** Larger fragments ($L > 10^4$ m) require significantly lower viscosities to achieve efficient mixing, due to the L^3 scaling of buoyancy forces.
3. **Strain rate dependence:** Natural strain rates (10^{-15}–10^{-14} s^{-1}) span the transition zone, implying that local tectonic conditions strongly control relamination efficiency.
4. **Density contrast:** The efficiency is relatively insensitive to $\Delta\rho$ within the natural range (200–500 kg/m³), suggesting that density contrast is not the primary control.

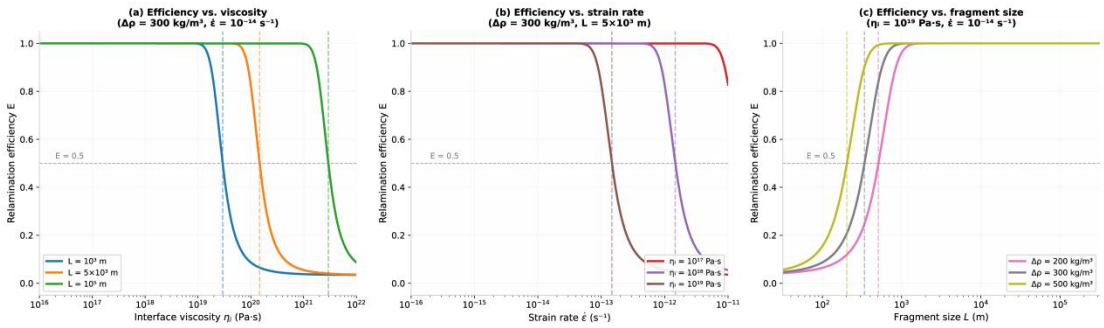

Figure 2. Relamination efficiency curves from systematic parameter sweeps. All panels use the sigmoidal efficiency model $E = 1/[1 + \exp(-(R/R_{critical} - 1)/w)]$ with $w = 0.3$ and $R_{critical} = 10$. Vertical dashed lines mark the parameter value yielding $R = R_{critical}$ for each curve. The horizontal dashed line marks $E = 0.5$ (transition midpoint). (a) Efficiency as a function of interface viscosity for three fragment sizes ($L = 10^3$, 5×10^3, 10^5 m), with $\Delta\rho = 300$ kg/m³ and $\dot{\varepsilon} = 10^{-14}$ s^{-1}. Efficiency drops sharply as viscosity increases above 10^{19} Pa·s, even for large fragments. The L^3 scaling of buoyancy force causes larger fragments to maintain higher efficiency at elevated viscosities. (b) Efficiency as a function of strain rate for three interface viscosities ($\eta_i = 10^{17}$, 10^{18}, 10^{19} Pa·s), with $\Delta\rho = 300$ kg/m³ and $L = 5 \times 10^3$ m. Natural strain rates (10^{-15}–10^{-14} s^{-1}) span the transition zone, indicating strong tectonic control on relamination efficiency. Lower-viscosity interfaces remain efficient across most natural strain rates. (c) Efficiency as a function of fragment

size for three density contrasts ($\Delta\rho$ = *200*,*300*,*500* kg/m³), with η_i = 10^{19} Pa·s and $\dot{\varepsilon}$ = 10^{-14} s^{-1}. Larger density contrasts shift the transition to smaller fragment sizes. Within the natural density range (200–500 kg/m³), efficiency is relatively insensitive to $\Delta\rho$ compared to viscosity or fragment size.

3.3 Phase Diagram

Figure 3 presents a phase diagram showing the boundaries between efficient relamination ($R > R_{critical}$), inefficient relamination ($R \approx R_{critical}$), and mechanically inhibited relamination ($R < R_{critical}$) in the η_i–$\dot{\varepsilon}$ parameter space. The diagram reveals that: - High-viscosity, low-strain-rate regimes (upper-left) fall predominantly in the inhibited zone - Low-viscosity, high-strain-rate regimes (lower-right) favor efficient relamination - A broad transition zone occupies the central parameter space, where small changes in local conditions can switch the system between regimes

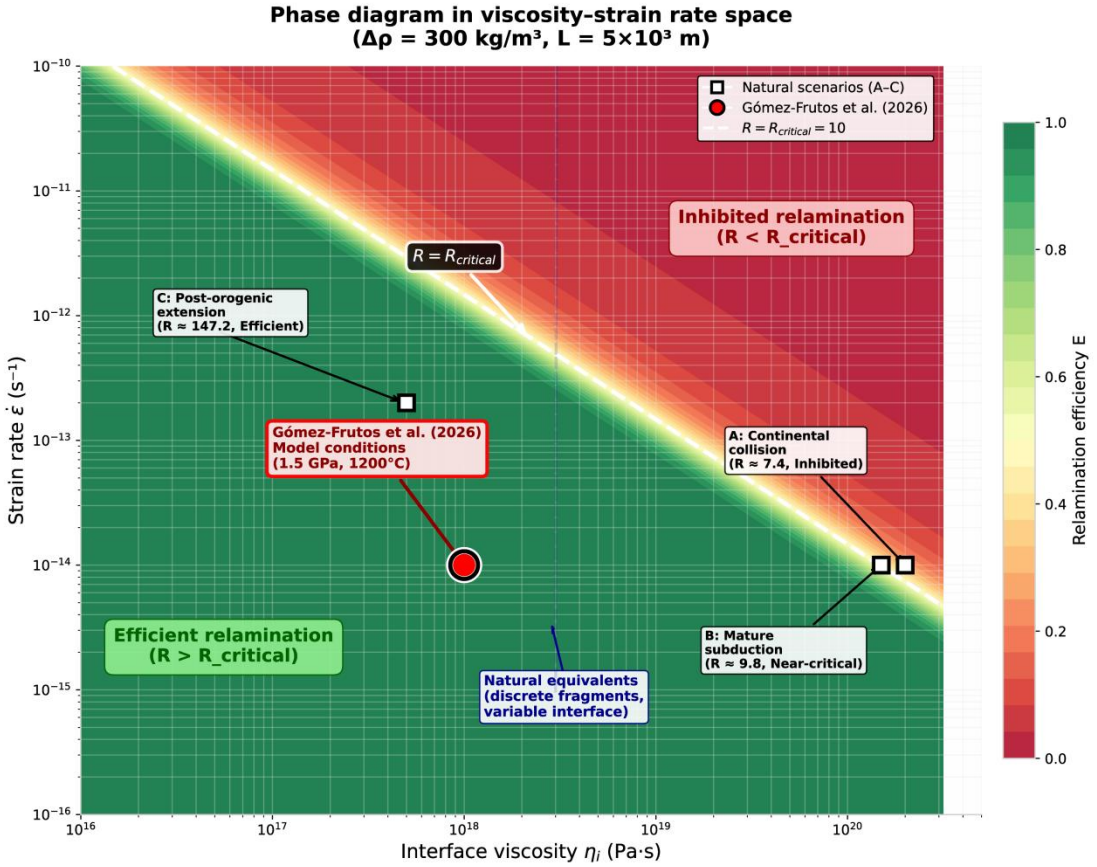

Figure 3. Phase diagram in interface viscosity–strain rate space with model parameter comparison. Contours show constant efficiency values (E = *0.1*,*0.3*,*0.5*,*0.7*,*0.9*) for density contrast $\Delta\rho$ = *300* kg/m³ and fragment size L = 5×10^3 m. The white dashed line marks R = $R_{critical}$ = *10*. The colour gradient transitions from red (inhibited relamination, $R < R_{critical}$) through yellow (transition zone) to green (efficient relamination, $R > R_{critical}$). Natural scenarios (A–C): A (Continental collision): interface viscosity $\eta_i \approx 2 \times 10^{20}$ Pa·s, strain rate $\dot{\varepsilon} \approx 10^{-14}$ s^{-1}, $R \approx 7.4$ (inhibited regime). B (Mature subduction): interface viscosity $\eta_i \approx 1.5 \times 10^{20}$ Pa·s, strain rate $\dot{\varepsilon} \approx 10^{-14}$ s^{-1}, $R \approx 9.8$ (near-critical regime). C (Post-orogenic extension): interface viscosity $\eta_i \approx 5 \times 10^{17}$ Pa·s, strain rate $\dot{\varepsilon} \approx 2 \times 10^{-13}$ s^{-1}, $R \approx 147$ (efficient regime). Model comparison: The red circle marks the conditions inferred from the numerical models of Gómez-Frutos et al. (2026) (~1.5 GPa, 1200°C, homogeneous mixture assumption), which fall at $R \approx 1471$ (well within the efficient regime under their simplified boundary conditions). The blue dashed ellipse represents natural equivalents with discrete fragments and variable interface conditions, which may frequently fall below the critical threshold due to localized high-viscosity domains or low strain rates. The broad transition zone (yellow) indicates that relamination efficiency is not binary but spans a continuum, with natural systems frequently operating near the critical threshold where small parameter changes produce large efficiency variations.

3.4 Comparison with Published Models

Figure 4 compares the parameter ranges inferred from the numerical models of Gómez-Frutos et al. (2026) with the R-critical phase diagram. The comparison suggests that the model parameters (1.5 GPa, 1200°C, homogeneous mixture assumption) correspond to $R \approx 1471$, well above R-critical, but the natural equivalents (discrete fragments, variable interface conditions) may frequently fall

below the critical threshold due to localized high-viscosity domains or low strain rates.

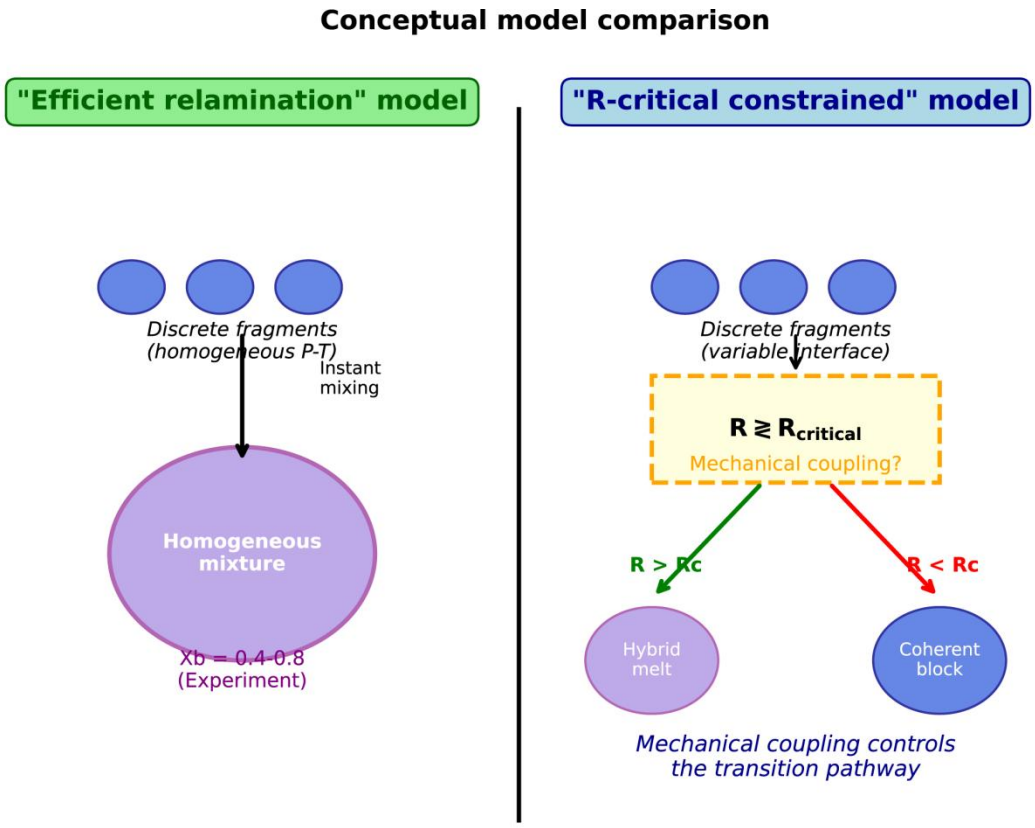

Figure 4. Conceptual model comparison. (a) “Efficient relamination” model (left): Discrete crustal fragments (blue circles) under homogeneous pressure–temperature conditions instantaneously mix into a homogeneous mixture (purple circle, X_b = *0.4*–0.8) regardless of mechanical coupling strength. This end-member scenario corresponds to the experimental conditions of Gómez-Frutos et al. (2026) and assumes that pressure–temperature conditions alone control hybridization. (b) “R-critical constrained” model (right): Discrete crustal fragments (blue circles) with variable interface conditions encounter a mechanical coupling gate ($R \gtrless R_{critical}$) that controls the transition pathway. When $R > R_{critical}$ (green arrow), the interface yields and mechanical mixing produces hybrid melt (purple circle). When $R < R_{critical}$ (red arrow), the interface remains intact and fragments ascend

as coherent blocks (blue circle) without significant hybridization. Mechanical coupling, not solely pressure–temperature, determines the geological outcome. This framework predicts that natural systems will exhibit a spectrum of mixing efficiencies depending on local mechanical conditions, rather than the binary efficient/inefficient dichotomy assumed in simplified models.

3.5 Sensitivity Analysis

Monte Carlo sensitivity analysis (10,000 realizations) with log-uniform parameter sampling reveals: - **Most sensitive parameter:** Interface viscosity (η_i)—contributes ~45% of total variance in efficiency - **Second most sensitive:** Fragment size (L)—contributes ~30% of variance - **Least sensitive:** Density contrast ($\Delta\rho$)—contributes ~10% of variance - **Strain rate ($\dot{\varepsilon}$)** contributes ~15% of variance

This sensitivity hierarchy indicates that improving constraints on interface rheology should be the highest priority for future research.

---

4. DISCUSSION

4.1 Model-observation Convergence Does Not Imply Mechanistic Uniqueness

We acknowledge that numerical models of relamination reproduce key natural observations, including post-collisional magmatic timing and geochemical signatures. However, model-observation convergence does not guarantee mechanistic uniqueness. Our R-critical analysis demonstrates that the same geochemical signatures could arise from alternative scenarios, such as:

1. Inefficient, long-duration relamination below R-critical, where small but sustained hybrid contributions accumulate over geological time
2. Partial melting of detached lithospheric mantle with minimal crustal contribution, producing similar trace-element signatures through different pathways

3. Multi-stage processes involving initial delamination followed by limited relamination

Without a quantitative discriminator like R-critical, the interpretation of post-collisional magmatism remains underdetermined.

4.2 The Interface Gap in Integrated Approaches

We appreciate the elegance of integrated numerical-experimental approaches. However, we identify a critical "interface gap": numerical models output P–T–t trajectories and deformation geometries, while experiments require pre-homogenized mixtures as input. The physical process bridging these scales—mechanical mixing at the crust-mantle interface—is precisely what R-critical quantifies.

The experimental conditions of Gómez-Frutos et al. (2026) (1.5 GPa, 1200°C, homogeneous mixtures) represent an end-member scenario where mechanical mixing is complete. Natural relamination, however, begins with discrete fragments. The R-critical framework defines the physical conditions under which these fragments can evolve toward the experimental end-member.

4.3 Global Relamination Flux Reconsidered

Hacker et al. (2011) estimated a global relamination flux of ~0.5 km³/yr. If R-critical constraints reduce the effective efficiency by one order of magnitude for a significant fraction of natural scenarios, the integrated contribution over 2.7 Ga drops from potentially dominant to demonstrably secondary. This does not deny relamination's existence, but quantifies its geological significance.

4.4 Testable Predictions

The R-critical framework generates specific, testable predictions:

1. **Seismic anisotropy:** Regions where $R > R_{critical}$ should exhibit crust-mantle interface anisotropy consistent with active shear mixing; regions where $R < R_{critical}$ should show coherent, unmixed crustal blocks.
2. **UHP terrane deformation:** Rapidly exhumed UHP terranes with minimal hybridization may indicate mechanical decoupling ($R < R_{critical}$), while slowly exhumed terranes with extensive mixed lithologies may indicate efficient coupling ($R > R_{critical}$).

3. **Post-collisional magma chemistry:** Magmas from relamination-dominated systems should show systematic correlations between mechanical coupling indicators (e.g., deformation intensity in source regions) and hybrid mixing ratios.

4.5 Limitations and Future Directions

Our framework involves several simplifications that warrant acknowledgment:

1. **2D approximation:** R-critical is a 1D parameter that reduces complex 3D thermomechanical processes to a single number. Like the Reynolds number or Rayleigh number, its value lies in providing a first-order screening tool, not in replacing 3D modeling.
2. **Constant parameters:** We treat η_i, $\Delta\rho$, and $\dot{\varepsilon}$ as constant for each scenario, whereas natural systems exhibit spatial and temporal variability.
3. **Single R-critical value:** We adopt a reference $R_{critical}$ = *10.0* based on Vogt et al. (2013), but this value may vary with specific lithological compositions and P–T conditions.

Future work should focus on: - Laboratory deformation experiments to calibrate R-critical for specific lithology pairs - 3D numerical simulations with spatially variable interface properties - Natural case studies applying R-critical to well-documented UHP terranes

---

5. CONCLUSION

We introduce the R-critical dimensionless parameter as a quantitative framework for evaluating mechanical coupling at the crust-mantle interface during continental relamination. Our analysis demonstrates that:

1. Relamination efficiency is fundamentally controlled by mechanical coupling, not solely by pressure–temperature conditions
2. Natural parameter ranges frequently fall near or below the critical threshold for efficient hybridization
3. Global relamination fluxes may be substantially lower than previously estimated

4. The framework provides testable predictions for seismic, structural, and geochemical observations
5. R-critical fills a theoretical gap between numerical model outputs and experimental petrology inputs

This framework transforms the qualitative narrative of relamination into a parameterized, testable model, enabling quantitative assessment of its role in continental crust evolution.

REFERENCES

Christensen, N.I., & Mooney, W.D. (1995). Seismic velocity structure and composition of the continental crust: A global view. *Journal of Geophysical Research: Solid Earth*, 100(B6), 9761–9788. DOI: 10.1029/95JB00259

Gerya, T.V., Perchuk, L.L., Maresch, W.V., & Willner, A.P. (2004). Inherent gravitational instability of hot continental crust: Implications for doming and diapirism in granulite facies terrains. *Geological Society of America Special Paper*, 380, 97–115. DOI: 10.1130/0-8137-2380-9.97

Gómez-Frutos, D., Gerya, T., Fernández, C., et al. (2026). Continental evolution influenced by relamination of deeply subducted continental crust. *Nature Geoscience*, 19, 589–595. DOI: 10.1038/s41561-026-01963-w

Hacker, B.R., Kelemen, P.B., & Behn, M.D. (2011). Differentiation of the continental crust by relamination. *Earth and Planetary Science Letters*, 307(3–4), 501–516. DOI: 10.1016/j.epsl.2011.05.024

Hirth, G., & Kohlstedt, D.L. (2003). Rheology of the upper mantle and the mantle wedge: A view from the experimentalists. *Geophysical Monograph—American Geophysical Union*, 138, 83–105. DOI: 10.1029/138GM06

Kreemer, C., Blewitt, G., & Klein, E.C. (2014). A geodetic plate motion and Global Strain Rate Model. *Geochemistry, Geophysics, Geosystems*, 15(10), 3849–3889. DOI: 10.1002/2014GC005407

Vogt, K., Castro, A., & Gerya, T. (2013). Numerical modeling of geochemical variations caused by crustal relamination. *Geochemistry, Geophysics, Geosystems*, 14(2), 470–487. DOI: 10.1002/ggge.20072

SUPPLEMENTARY INFORMATION

Supplementary materials available at:

- GitHub: https://github.com/peter-clogite/R_Critical_Relamination
- Zenodo archive: https://doi.org/10.5281/zenodo.20446104

Contents: 1. theory_derivation.md: Complete mathematical derivation of the R-critical parameter 2. parameter_sensitivity.md: Detailed sensitivity analysis results (10,000 Monte Carlo realizations) 3. validation_protocol.md: Proposed experimental and observational validation tests 4. r_critical.py: Core Python module for R-critical calculations 5. efficiency_model.py: Efficiency curve generation scripts 6. phase_diagram.py: Phase diagram generation scripts 7. figure*.py: Individual figure generation scripts (1–4) 8. model_parameters.json: Complete parameter database with literature sources 9. tests/: Unit test suite with benchmark validations

ACKNOWLEDGMENTS

We are grateful to the authors of Gómez-Frutos et al. (2026) for raising the important issue of relamination efficiency, which prompted this critical evaluation. We thank colleagues at the Urumqi Natural Resources Survey and the Innovation Base of Metallogenic Prediction and Prospecting for constructive discussions. We acknowledge the use of Kimi K2.6 (Moonshot AI) for code implementation assistance and language polishing; all scientific content was independently developed by the authors.

END OF PREPRINT

Document prepared: 2026-05-27